A&A 463, 23–29 (2007)
DOI: 10.1051/0004-6361:20066344


Astronomy & Astrophysics

# Flow instabilities of magnetic flux tubes

## I. Perpendicular flow

M. Schüssler[1] and A. Ferriz Mas[2,3]

[1] Max-Planck-Institut für Sonnensystemforschung, 37191 Katlenburg-Lindau, Germany
e-mail: msch@mps.mpg.de
[2] Dept. de Física Aplicada, Facultad de Ciencias de Orense, Universidad de Vigo, 32004 Orense, Spain
[3] Astronomy Division, Faculty of Physical Sciences, University of Oulu, 90014 Oulu, Finland
e-mail: antonio.ferriz@oulu.fi

Received 4 September 2006 / Accepted 8 November 2006

**ABSTRACT**

*Context.* The stability properties of filamentary magnetic structures are relevant for the storage and dynamics of magnetic fields in stellar convection zones and possibly also in other astrophysical contexts.
*Aims.* In a series of papers we study the effect of external and internal flows on the stability of magnetic flux tubes. In this paper we consider the effect of a flow perpendicular to a straight, horizontal flux tube embedded in a gravitationally stratified fluid. The flow acts on the flux tube by exerting an aerodynamic drag force and by modifying the pressure stratification in the background medium.
*Methods.* We carry out a Lagrangian linear stability analysis in the framework of the approximation of thin magnetic flux tubes.
*Results.* The external flow can drive monotonic and oscillatory instability (overstability). The stability condition depends on direction and magnitude of the external velocity as well as on its first and second derivatives with respect to depth. The range of the flow-driven instabilities typically extends to modes with much shorter wavelengths than for the buoyancy-driven undulatory Parker instability.
*Conclusions.* Perpendicular flows with Alfvénic Mach number of order unity can drive monotonic as well as oscillatory instability of thin magnetic flux tubes. Such instability can affect the storage of magnetic flux in stellar interiors.

**Key words.** magnetic fields – magnetohydrodynamics (MHD) – Sun: magnetic fields – stars: magnetic fields

## 1. Introduction

Astrophysical magnetic fields become highly structured and intermittent when they are embedded in an electrically conducting plasma in turbulent motion with high magnetic Reynolds number. A typical example are the magnetic fields in stellar convection zones, but also fields in accretion disks and in the interstellar medium most probably occur in a filamentary state (e.g., Schramkowski & Torkelsson 1996; Hanasz & Lesch 2001). Physical processes involving magnetic flux filaments are often studied in the context of the approximation of thin magnetic flux tubes, whereby the filaments are treated as bundles of magnetic field lines whose diameter is small compared to all other relevant length scales and which are separated from their (non-magnetic or more weakly magnetized) environment by a tangential discontinuity in ideal magnetohydrodynamics (Roberts & Webb 1978; Spruit 1981; Ferriz-Mas & Schüssler 1989).

The stability properties of magnetic flux filaments in the presence of flows are relevant in various astrophysical situations, for instance in connection with magneto-convection and the storage of magnetic flux in stellar interiors (e.g., Schüssler 1984a; Vishniac 1995) and accretion disks (Schramkowski 1996), for the maintainance of magnetic structures in stellar atmospheres (Schüssler 1984b), or for collimated outflows and jets (Ferrari 1998).

In a series of papers we will present a systematic study of the stability of thin flux tubes in the presence of (internal or external) flows, excluding azimuthal flows around the flux tube (see, e.g., Kolesnikov et al. 2004). In the present paper we consider flows directed perpendicular to the flux tube in plane-parallel geometry. A subsequent paper will be concerned with the effect of longitudinal flows directed parallel to the field lines of the equilibrium flux tube. While these analyses are mainly devoted to the general properties and physical mechanisms of the relevant instabilities, in a third paper we will apply the results to the specific case of flux tubes stored near the bottom of the solar convection zone.

## 2. Flux tubes subject to perpendicular flows

In this paper, we consider an external flow directed perpendicularly to the axis of a thin magnetic flux tube. The plasma is diverted by the flux tube, flows round it and exerts an aerodynamic drag force (Parker 1975, 1979, Chap. 8) arising from a pressure difference between the upstream and downstream sides of the interface between flux tube and environment. Therefore, only the perpendicular component contributes to the drag force in the case of an arbitarily directed external flow. A small perpendicular displacement of the flux tube can grow and lead to instability if the restoring force (e.g., due to magnetic tension or to the stratification of the external medium) is overcome by a sufficiently enhanced drag force (e.g., due to an acceleration of the external flow or a change of the tube radius). Note that the simple description of the interaction between the flux tube and an external flow via the concept of a drag force does not permit to consider phenomena like vortex shedding or a turbulent wake, which may well affect the dynamics of a flux tube (e.g., Emonet et al. 2001; Cheung et al. 2006).

The stability of flux tubes in external flows has been considered previously by van Ballegooijen & Choudhuri (1988), who studied the effect of a meridional flow on a toroidal flux tube (a flux ring) located in a plane parallel to the equator of a spherical star. Here we consider straight, horizontal flux tubes embedded in a plane-parallel stratified fluid and subject to vertical flows, thus extending previous work (Schüssler 1990). The stability of a toroidal flux tube in a radially directed flow will be analyzed in a subsequent paper. While the formalism of the linear stability analysis is developed in a quite general form, the discussion of the results focuses upon the conditions prevailing in the deep parts of solar/stellar convection zones, i.e., low Mach numbers of the flows and large values of the plasma $\beta$.

## 3. Equilibrium

Consider a horizontal, untwisted magnetic flux tube embedded in a stratified medium with constant gravitational acceleration, $\boldsymbol{g} = -g\,\boldsymbol{e}_z$, where $\boldsymbol{e}_z$ is the unit vector in the upward direction and $g > 0$. Assuming a height-dependent vertical flow, $\boldsymbol{u}_\mathrm{e} = U(z)\,\boldsymbol{e}_z$, the stationary pressure stratification of the external medium is given by

$$\frac{\mathrm{d}p_\mathrm{e}}{\mathrm{d}z} = -\rho_\mathrm{e}\left(g + U\,\frac{\mathrm{d}U}{\mathrm{d}z}\right), \tag{1}$$

where $p_\mathrm{e}(z)$ and $\rho_\mathrm{e}(z)$ are the pressure and density profiles, respectively, in the external medium.

The equilibrium flux tube is located at height $z = z_0$ and taken to be uniform in the tangential (horizontal) direction. For a thin flux tube whose geometry is described by the Frenet basis vectors (e.g., Ferriz-Mas & Schüssler 1993), the force equilibrium in the normal (vertical) direction is given by

$$(\rho_0 - \rho_\mathrm{e0})\,g - \rho_\mathrm{e0}\,U_0\left(\frac{\mathrm{d}U}{\mathrm{d}z}\right)_0 + \boldsymbol{F}_\mathrm{D0}\cdot\boldsymbol{e}_\mathrm{n0} = 0, \tag{2}$$

where $\boldsymbol{F}_\mathrm{D0}$ is the drag force (per unit length) on the tube due to the external flow. The unit normal vector, $\boldsymbol{e}_\mathrm{n0} = -\boldsymbol{e}_z$, is assumed to be directed downward, i.e., along the direction of the gravitational acceleration. The index "0" indicates equilibrium quantities in the interior of the flux tube, such as $\rho_0$, as well as external quantities at the equilibrium height, such as $\rho_\mathrm{e0} = \rho_\mathrm{e}(z_0)$. The force equilibrium in the horizontal plane, i.e. in the tangential and binormal directions, is trivially fulfilled for a straight, uniform and horizontal tube.

The drag force is given by

$$\boldsymbol{F}_\mathrm{D0} = \mathrm{sgn}(U_0)\frac{C_\mathrm{D}\,\rho_\mathrm{e0}U_0^2}{\pi a_0}\boldsymbol{e}_z \equiv -F_\mathrm{D0}\,\boldsymbol{e}_z, \tag{3}$$

where $a_0$ is the equilibrium radius of the flux tube and $C_\mathrm{D}$ is the dimensionless drag coefficient, generally considered to be of order unity for flows with high Reynolds number (e.g., Batchelor 1967, Chap. 5.11). We have chosen the sign of $F_\mathrm{D0}$ such that this quantity is positive for downflows ($U_0 < 0$). Dividing Eq. (2) by $\rho_\mathrm{e0}\,g$, we obtain

$$\frac{\rho_0}{\rho_\mathrm{e0}} = 1 + \frac{U_0}{g}\left(\frac{\mathrm{d}U}{\mathrm{d}z}\right)_0 - \frac{F_\mathrm{D0}}{\rho_\mathrm{e0}g} \equiv 1 + \epsilon - \chi, \tag{4}$$

where $\epsilon$ is the (signed) Froude number (i.e., ratio of inertial force to gravity) and $\chi$ represents the ratio of the drag force to gravity. Clearly, an equilibrium can only exist if the r.h.s. of Eq. (4) is positive. For the conditions prevailing in the lower solar convection zone, $\epsilon$ and $\chi$ are small quantities. We introduce the local adiabatic sound speed, $c_\mathrm{se}$, and the the local pressure scale height, $H_{p\mathrm{e}} = c_\mathrm{se}^2/(\gamma g)$, in the external medium (assumed to be an ideal gas) at the position of the equilibrium flux tube, where $\gamma$ is the ratio of the specific heats. This allows us to write the Froude number in the form

$$\epsilon = \frac{U_0}{g}\left(\frac{\mathrm{d}U}{\mathrm{d}z}\right)_0 = \gamma\left(\frac{U_0}{c_\mathrm{se}}\right)^2\left(\frac{H_{p\mathrm{e}}}{H_U}\right), \tag{5}$$

where $H_U \equiv U_0/(\mathrm{d}U/\mathrm{d}z)_0$ is the local scale height of the external velocity field. Note that $H_U$ can have either sign, while $H_{p\mathrm{e}} > 0$ by definition. The first ratio on the r.h.s. of Eq. (5), the square of the Mach number, is of the order of $10^{-3}$, while the second ratio is of order unity for the convective flows in the lower solar convection zone. As a consequence, we have $|\epsilon| \ll 1$. Similarly, we can write

$$\chi = -\mathrm{sgn}(U_0)\frac{\gamma\,C_\mathrm{D}}{\pi}\left(\frac{U_0}{c_\mathrm{se}}\right)^2\left(\frac{H_{p\mathrm{e}}}{a_0}\right). \tag{6}$$

With $(U_0/c_\mathrm{se})^2 \simeq 10^{-6}$ we find that $|\chi| \ll 1$ unless the tube radius is much smaller than one km.

Note that a stationary equilibrium of the kind described by Eq. (2) requires a non-vanishing buoyancy force unless the two flow-related terms happen to balance each other, which would require a rather unrealistic fine-tuning.

The force equilibrium of a thin flux tube is complemented by the condition of instantaneous lateral pressure balance,

$$p_\mathrm{e0} = p_0 + \frac{B_0^2}{8\pi}, \tag{7}$$

where $B_0$ is the magnetic field strength of the equilibrium flux tube.

## 4. Linear stability analysis

Following previous work (e.g., Spruit & van Ballegooijen 1982; Schüssler 1990; Ferriz-Mas & Schüssler 1993, 1995; Schmitt 1998) we consider a Lagrangian perturbation of the flux tube. The corresponding displacement vector, $\boldsymbol{\xi}$, is expressed in terms of the Frenet basis, $\{\boldsymbol{e}_\mathrm{t0}, \boldsymbol{e}_\mathrm{n0}, \boldsymbol{e}_\mathrm{b0}\}$, in the tangential, normal, and binormal directions along the unperturbed path of the flux tube,

$$\boldsymbol{\xi}(s_0, t) = \xi_\mathrm{t}\boldsymbol{e}_\mathrm{t0} + \xi_\mathrm{n}\boldsymbol{e}_\mathrm{n0} + \xi_\mathrm{b}\boldsymbol{e}_\mathrm{b0}, \tag{8}$$

where the components of $\boldsymbol{\xi}$ are functions of time, $t$, and of the arc length, $s_0$, along the equilibrium flux tube. We take $s_0$ as Lagrangian coordinate. The direction of $\boldsymbol{e}_\mathrm{t0}$ is defined to be parallel to the unperturbed field vector, $\boldsymbol{B}_0$. The tangential and normal components of the momentum equation for the perturbed thin flux tube are given by

$$\rho\,\ddot{\xi}_\mathrm{t} = \frac{\partial}{\partial s}\left(\frac{B^2}{8\pi}\right) + (\rho - \rho_\mathrm{e})\boldsymbol{g}\cdot\boldsymbol{e}_\mathrm{t} + \rho_\mathrm{e}[(\boldsymbol{u}_\mathrm{e}\cdot\nabla)\boldsymbol{u}_\mathrm{e}]\cdot\boldsymbol{e}_\mathrm{t} \tag{9}$$

and

$$\mu\,\rho\,\ddot{\xi}_\mathrm{n} = \frac{B^2}{4\pi r} + (\rho - \rho_\mathrm{e})\boldsymbol{g}\cdot\boldsymbol{e}_\mathrm{n} + \rho_\mathrm{e}[(\boldsymbol{u}_\mathrm{e}\cdot\nabla)\boldsymbol{u}_\mathrm{e}]\cdot\boldsymbol{e}_\mathrm{n} + \boldsymbol{F}_\mathrm{D}\cdot\boldsymbol{e}_\mathrm{n}, \tag{10}$$

where the dots indicate time derivatives at constant Lagrangian coordinate $s_0$. The numerical factor $\mu$ takes account of the enhanced inertia of the flux tube with respect to transversal acceleration, which arises from the required co-acceleration of fluid

in the environment (Spruit 1981; Moreno-Insertis et al. 1996). $r$ is the radius of curvature of the flux tube path (for a straight equilibrium tube we have $r_0 \to \infty$). The binormal component of the momentum equation is decoupled from the other equations and its linearized form describes solely a drag-damped tube wave (i.e., the thin flux tube version of the MHD slow wave, cf. Defouw 1976; Ryutov & Ryutova 1976), so that we do not consider it further.

We write all quantities as the sum of their equilibrium values plus the (Lagrangian) perturbations due to the displacement $\boldsymbol{\xi}$ and linearize Eqs. (9) and (10) by ignoring all terms that are quadratic or of higher order in the perturbations. Using the equilibrium condition given by Eq. (4) and writing all perturbations in terms of the components of the displacement vector (see, e.g., Spruit & van Ballegooijen 1982; Ferriz-Mas & Schüssler 1993), we obtain for the tangential acceleration

$$\ddot{\xi}_\mathrm{t} = c_\mathrm{T}^2 \frac{\partial^2 \xi_\mathrm{t}}{\partial s_0^2} + \left[\frac{c_\mathrm{T}^2(1+\epsilon) - c_\mathrm{S}^2\chi}{\gamma H_p (1+\epsilon-\chi)}\right]\frac{\partial \xi_\mathrm{n}}{\partial s_0}, \tag{11}$$

where we have assumed isentropic perturbations. The quantities $H_p = p_0/(\rho_0 g)$ and $c_\mathrm{S} = (\gamma p_0/\rho_0)^{1/2}$ are the scale height and the sound velocity, respectively, based on the equilibrium quantities within the flux tube; $c_\mathrm{A} = B_0/(4\pi\rho)^{1/2}$ is the Alfvén speed and $c_\mathrm{T} = c_\mathrm{S} c_\mathrm{A}/(c_\mathrm{S}^2 + c_\mathrm{A}^2)^{1/2}$ is the tube (or cusp) speed. Taking the limit $\beta \equiv 8\pi p_0/B_0^2 = 2c_\mathrm{S}^2/(\gamma c_\mathrm{A}^2) \gg 1$, which is revelant for the conditions in the deep solar convection zone, together with the limits $\epsilon \ll 1$ and $\chi \ll 1$ (but retaining the product $\beta\chi$), we obtain from Eq. (11)

$$\ddot{\xi}_\mathrm{t} = c_\mathrm{A}^2 \frac{\partial^2 \xi_\mathrm{t}}{\partial s_0^2} + \frac{c_\mathrm{A}^2}{2H_p}\left(\frac{2}{\gamma} - \beta\chi\right)\frac{\partial \xi_\mathrm{n}}{\partial s_0}. \tag{12}$$

After subtracting the equilibrium condition and linearizing, the normal component of the equation of motion, Eq. (10), is written as

$$\begin{aligned}\mu\rho_0 \ddot{\xi}_\mathrm{n} &= \frac{B_0^2}{4\pi}\frac{\partial^2 \xi_\mathrm{n}}{\partial s_0^2} + (\rho_1 - \rho_{\mathrm{e}1})g + \frac{\rho_{\mathrm{e}0}}{2}\left(U_0^2\right)'' \xi_\mathrm{n} \\ &\quad - \rho_{\mathrm{e}1} U_0 U_0' + F_{\mathrm{D}0}\left[\frac{B_1}{2B_0} + \frac{\rho_{\mathrm{e}1}}{\rho_{\mathrm{e}0}} - \frac{2(U_0'\xi_\mathrm{n} - \dot{\xi}_\mathrm{n})}{U_0}\right],\end{aligned} \tag{13}$$

where the dashes indicate derivatives with respect to $z$ (height), taken at the equilibrium position, $z = z_0$, of the flux tube. The subscript "1" denotes the perturbations. The third and the fourth term on the r.h.s. represent the perturbations of the inertial force, while the last term results from the perturbation of the drag force. Writing all perturbations in terms of the components of $\boldsymbol{\xi}$, we obtain after some lengthy, but straightforward, algebra:

$$\begin{aligned}\mu\ddot{\xi}_\mathrm{n} &+ \left(\frac{2C_\mathrm{D}|U_0|}{\pi a_0}\frac{\rho_{\mathrm{e}0}}{\rho_0}\right)\dot{\xi}_\mathrm{n} = c_\mathrm{A}^2\frac{\partial^2 \xi_\mathrm{n}}{\partial s_0^2} \\ &+ \frac{c_\mathrm{T}^2}{2H_p}\left(-\frac{2}{\gamma} + \frac{\beta\chi}{2}\frac{\rho_{\mathrm{e}0}}{\rho_0}\right)\frac{\partial \xi_\mathrm{t}}{\partial s_0} + T\xi_\mathrm{n},\end{aligned} \tag{14}$$

where

$$\begin{aligned}T \equiv \frac{\rho_{\mathrm{e}0}}{\rho_0}\Bigg[&(-1-\epsilon+\chi)\frac{(1-\nabla)(1+\epsilon)g}{H_{p\mathrm{e}}} + \frac{(1+\epsilon)g c_\mathrm{T}^2}{\gamma c_\mathrm{A}^2 H_p} \\ &+ \frac{1}{2}\left(U_0^2\right)'' + \chi g\left(\frac{(1+\epsilon)c_\mathrm{T}^2}{2\gamma c_\mathrm{A}^2 H_p} - \frac{2U_0'}{U_0}\right)\Bigg]\end{aligned} \tag{15}$$

and $\nabla = (\mathrm{d}\ln T_\mathrm{e}/\mathrm{d}\ln p_\mathrm{e})_0$ is the logarithmic temperature gradient at the equilibrium position of the flux tube. $\nabla_\mathrm{ad}$ is the corresponding value of $\nabla$ for a homentropic ("adiabatic") stratification. We introduce the "superadiabaticity" $\delta \equiv \nabla - \nabla_\mathrm{ad}$. For an ideal gas we have $\nabla_\mathrm{ad} = (\gamma-1)/\gamma$ and thus $1 - \nabla = 1/\gamma - \delta$. Considering the limits $\delta, \epsilon, \chi \ll 1, \beta \gg 1$ and retaining products of the small quantities with $\beta$, we obtain

$$\begin{aligned}\mu\ddot{\xi}_\mathrm{n} &+ \left(\frac{2C_\mathrm{D}|U_0|}{\pi a_0}\right)\dot{\xi}_\mathrm{n} = c_\mathrm{A}^2\frac{\partial^2 \xi_\mathrm{n}}{\partial s_0^2} + \frac{c_\mathrm{A}^2}{2H_p}\left(-\frac{2}{\gamma} + \frac{\beta\chi}{2}\right)\frac{\partial \xi_\mathrm{t}}{\partial s_0} \\ &+ \frac{c_\mathrm{A}^2}{2H_p^2}\left[-\frac{2}{\gamma}\left(\frac{1}{\gamma} - \frac{1}{2}\right) + \beta\delta + \beta I + \beta D\right]\xi_\mathrm{n},\end{aligned} \tag{16}$$

with

$$\beta I \equiv \frac{H_p^2}{c_\mathrm{A}^2}\left(U_0^2\right)'' = H_p^2\left(M_\mathrm{A}^2\right)'' = M_\mathrm{A}^2\left[2 - (H_U)'\right]\left(\frac{H_p}{H_U}\right)^2, \tag{17}$$

where $M_\mathrm{A}^2 = U_0^2/c_\mathrm{A}^2$ is the Alfvénic Mach number,

$$\beta D \equiv \beta\chi\left(\frac{1}{2\gamma} - \frac{2H_p}{H_U}\right), \tag{18}$$

and

$$\beta\chi = -\mathrm{sgn}(U_0)\left(\frac{2C_\mathrm{D}}{\pi}\right)\left(\frac{H_p}{a_0}\right)M_\mathrm{A}^2\,. \tag{19}$$

We cast Eqs. (12) and (16) in dimensionless form by taking $\sqrt{2}H_p/c_\mathrm{A}$ as the unit of time and $H_p$ as the length unit. Using the same symbols as before for the dimensionless quantities, we then have

$$\ddot{\xi}_\mathrm{t} = 2\frac{\partial^2 \xi_\mathrm{t}}{\partial s_0^2} + \left(\frac{2}{\gamma} - \beta\chi\right)\frac{\partial \xi_\mathrm{n}}{\partial s_0}, \tag{20}$$

and

$$\begin{aligned}\mu\ddot{\xi}_\mathrm{n} &+ R\dot{\xi}_\mathrm{n} = 2\frac{\partial^2 \xi_\mathrm{n}}{\partial s_0^2} + \left(-\frac{2}{\gamma} + \frac{\beta\chi}{2}\right)\frac{\partial \xi_\mathrm{t}}{\partial s_0} \\ &+ \left[-\frac{2}{\gamma}\left(\frac{1}{\gamma} - \frac{1}{2}\right) + \beta\delta + \beta I + \beta D\right]\xi_\mathrm{n},\end{aligned} \tag{21}$$

with

$$R \equiv \left(\frac{2\sqrt{2}C_\mathrm{D}}{\pi}\right)\left(\frac{H_p}{a_0}\right)|M_\mathrm{A}|\,. \tag{22}$$

Taking Fourier components of the form $\xi_\mathrm{n} \propto \exp(\mathrm{i}ks_0 - \mathrm{i}\omega t)$ with real wavenumber $k$ and complex frequency $\omega$, leads to the dispersion relation

$$\mu\omega^4 + \mathrm{i}c_3\omega^3 + c_2\omega^2 + \mathrm{i}c_1\omega + c_0 = 0 \tag{23}$$

with

$$c_3 = R, \tag{24}$$

$$c_2 = -2k^2(\mu+1) - \frac{2}{\gamma}\left(\frac{1}{\gamma} - \frac{1}{2}\right) + \beta\delta + \beta I + \beta D, \tag{25}$$

$$c_1 = -2k^2 R, \tag{26}$$

$$c_0 = -2k^2\left[-2k^2 + \frac{1}{\gamma} + \beta\delta + \beta I - \beta\chi\left(\frac{1}{\gamma} + \frac{2H_p}{H_U} - \frac{\beta\chi}{4}\right)\right]. \tag{27}$$

## 5. Instabilities

We first consider some special cases, before we proceed to discuss the dispersion relation in the general case.

### 5.1. No flow

In the static case, we recover the dispersion relation of Spruit & van Ballegooijen (1982). The criterion for the onset of the monotonic undulatory (or Parker) instability is

$$\beta\delta + \frac{1}{\gamma} - 2k^2 > 0\,. \tag{28}$$

### 5.2. No drag

If we ignore the drag force, we have $R = D = \chi = 0$ and the only effect of the external flow results from the inertial term in the force equilibrium of the external medium, Eq. (1). The dispersion relation then has the same form as the corresponding equation in the static case, with the superadiabaticity replaced by an "effective" value $\delta \to \delta + I$, resulting in the criterion

$$\beta\left[\delta + H_p^2\left(M_\mathrm{A}^2\right)''\right] + \frac{1}{\gamma} - 2k^2 > 0 \tag{29}$$

for instability. The effect of the new term depends on the sign of $(M_\mathrm{A}^2)''$: a positive value is destabilizing, i.e. increases the effective superadiabaticity of the external stratification, while a negative value has a stabilizing effect. We see from Eq. (17) that $\beta I$ is positive (and thus destabilizing) as long as $(H_U)' < 2$. From a physical point of view, the influence of the quantity $\beta I$ on the stability properties results from the effect of the inertial force on the external pressure gradient given in Eq. (1): a positive value of $\beta I$ leads to a steepening of the pressure gradient with height, equivalent to the effect of a stronger temperature decrease with height. A sufficiently large steepening of the pressure gradient leads to buoyancy-driven instability.

### 5.3. Purely vertical displacement (k = 0)

In the case $k = 0$ we have $c_0 = c_1 = 0$ and the dispersion relation (for $\omega \neq 0$) becomes a quadratic equation with the roots

$$\omega_\pm = -\frac{iR}{2\mu} \pm \left(\frac{\omega_\mathrm{I}^2}{\mu} - \frac{R^2}{4\mu^2}\right)^{1/2}, \tag{30}$$

where

$$\omega_\mathrm{I}^2 \equiv \omega_0^2 - \beta I - \beta D = \frac{2}{\gamma}\left(\frac{1}{\gamma} - \frac{1}{2}\right) - \beta\left(\delta + I + D\right) \tag{31}$$

and $\omega_0$ is the "magnetic Brunt-Väisälä frequency" (cf. Moreno-Insertis et al. 1992). For $\omega_\mathrm{I}^2 > 0$, the system is stable and represents the elementary case of a damped oscillator with exponentially or oscillatory decaying amplitude, depending on the sign of the expression under the square root. In the case $\omega_\mathrm{I}^2 < 0$, the solution $\omega_+$ has a vanishing real part and a positive imaginary part, indicating monotonic instability. The criterion for instability, $\omega_\mathrm{I}^2 < 0$, again is formally the same as the corresponding criterion in the static case (Spruit & van Ballegooijen 1982), if we replace the superadiabaticity through $\delta \to \delta + I + D$.

The effect of $I$ on the stability is the same as in the previous case: the sign of $(M_\mathrm{A}^2)''$ determines whether the term is stabilizing or destabilizing. As Eqs. (18) and (19) show, the effect of the drag term in Eq. (31) depends on the signs of both $U(z)$ and its height gradient. For instance, for a flow with constant mass flux density, $\rho_\mathrm{e}U$, in an isothermal medium, we have $H_U = -H_p$, so that the term in brackets in Eq. (18) is always positive and the sign of $\beta D$ then depends only on the direction of the flow. Under these conditions, an upflow ($\chi < 0$) leads to $\beta D < 0$ and therefore is stabilizing, while a downflow has a destabilizing effect. This behavior can be understood physically through the changes in tube radius and external density due to the displacement. An upward displacement leads to an expansion of the flux tube and a decrease of $\rho_\mathrm{e}$, so that the drag force decreases (cf. Eq. (3)). Similarly, for a downward displacement we find an increase of the drag force. If we now have a flux tube in equilibrium with a downflow, for both upward and downward displacements the perturbation of the drag force tends to increase the displacement and thus favors instability, while the reverse is true for an upflow. In the case $H_U > 0$, corresponding to an accelerating upflow or downflow, the drag force changes such that it supports the growth of the displacement and thus favors instability, while $H_U < 0$ has a stabilizing effect.

### 5.4. General case: monotonic instability

In the case of Eqs. (23)–(27), the well-known analytic procedure to solve a quartic equation leads to lengthy and cumbersome expressions, which do not provide much insight into the physical conditions leading to instability or otherwise. We therefore discuss some specific properties of the general dispersion relation. Rewriting Eq. (23) in terms of $\tilde{\omega} \equiv -\mathrm{i}\omega$, we obtain a quartic equation with real coefficients, so that Descartes' sign rule can be applied: *the number of positive, real roots of a polynomial with real coefficients is smaller than or equal to the number of sign changes in the sequence of its coefficients. The difference is an even number.* A real root $\tilde{\omega} > 0$ entails a purely imaginary value of $\omega$ with $Im(\omega) > 0$, which means monotonic instability.

It is easy to see from the sign rule that a sufficient criterium for monotonic instability is given by $c_0 < 0$. Inspection of Eq. (27) shows that this condition is always fulfilled for sufficiently large values of $\beta\chi$ since the term $(\beta\chi)^2/4$ then dominates in the expression for $c_0$. This is also evident from Fig. 1, which shows the real part (full lines) and the imaginary part (dashed lines) of the complex frequency, $\omega$, as a function of $M_\mathrm{A}$ for the case $\mu = 2$, $k = 1$, $H_p/a_0 = 10$, $H_p/H_U = 0$ (i.e., height-independent external velocity), $\omega_0^2 = 0.5$, $C_D = 1$, and $\gamma = 5/3$. These values are chosen to roughly correspond to the conditions in the subadiabatic overshoot layer below the solar convection zone proper. They describe a flux tube equilibrium that is stable in the absence of an external flow. Figure 1 displays only the two modes relevant for monotonic instability. For sufficiently large flow speed ($M_\mathrm{A} > 0.52$ or $M_\mathrm{A} < -0.81$), we find a positive imaginary part of $\omega$, indicating instability. The two modes are oscillatory for $-0.46 < M_\mathrm{A} < 0.37$, at which positions they merge and become monotonic. Owing to the overall damping effect described by the terms containing the quantity $R$, the merging of the oscillatory modes does not immediately lead to an unstable monotonic mode (as in the case without drag): a somewhat larger flow speed is required to overcome the damping effect.

The dependence of the stability criterion on wavenumber $k$ for the same case is illustrated in Fig. 2, which gives contour lines of the imaginary part of the frequency for $Im(\omega) > 0$. We find from Eq. (28) that in the range $0 < k < 0.33$, the buoyancy-driven undular instability sets in for $M_\mathrm{A} = 0$. Within a certain

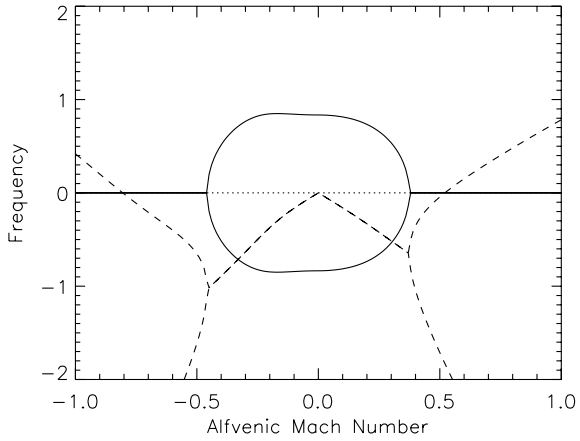


**Fig. 1.** Monotonic instability in the case $\mu = 2$, $k = 1$, $H_p/a_0 = 10$, $H_p/H_U = 0$, $\omega_0^2 = 0.5$, $C_D = 1$. The full and dashed lines give the real and imaginary parts, respectively, of the (dimensionless) frequency, $\omega$, as functions of the Alfvénic Mach number, $M_A$, of the perpendicular external flow. Instability sets in for sufficiently large flow speed, when the imaginary part of $\omega$ becomes positive for one of the modes. For somewhat smaller values of $|M_A|$, the oscillatory modes merge and transform into a pair of monotonic modes.

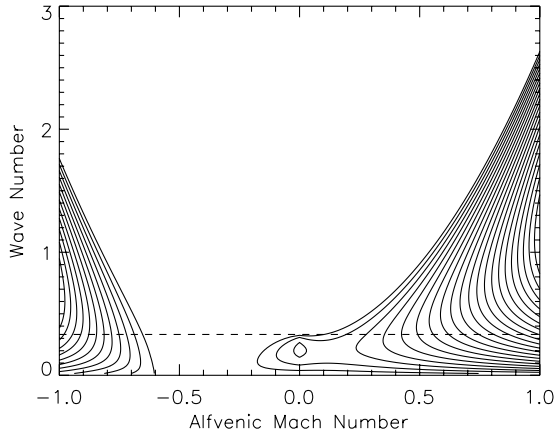


**Fig. 2.** Contours of equal growth rate (positive imaginary part of $\omega$) of the unstable monotonic modes on the $M_A$-$k$ plane for the same case as in Fig. 1. For a given (and sufficiently large) value of the flow speed, the monotonic instability prevails up to a critical wavenumber. The dashed horizontal line indicates the value $k = 0.33$, below which the buoyancy-driven Parker instability sets in for $M_A = 0$. A downflow within a certain range of speeds can stabilize the monotonic modes for all values of $k$.

range of flow speeds, a downflow can stabilize the flux tube for all values of $k$.

The physical mechanisms acting in the case of finite wavelength perturbations are more involved than in the case of purely vertical displacements. Buoyancy-driven instability is facilitated by the sliding of matter from the crests to the troughs of the perturbed flux tube, leading to a density reduction in the former and to a density enhancement in the latter regions. The perturbation of the internal density is proportional to the equilibrium density, $\rho_0$ (see, e.g., Spruit & van Ballegooijen 1982; Ferriz-Mas & Schüssler 1993; Schüssler 1990, Chap. 5.7.3), so that (for unchanged external density stratification) an increase of the equilibrium density has a destabilizing effect while a decrease has a stabilizing tendency. According to the equilibrium condition given by Eq. (4), an external downflow leads to a (stabilizing) decrease of $\rho_0$ while the opposite is true for an external upflow. Consequently, the (indirect) effect of an external flow on the buoyancy-driven instability for finite-wavelength perturbations is opposite to its direct effect via the perturbation of the drag force in the case of purely vertical displacements discussed in Sect. 5.3. This is the reason why, in the case of a downflow, instability requires higher flow speeds than in the in the case $k = 0$ discussed in the previous subsection, for which instability sets in already for $M_A < -0.51$. For sufficiently fast downflows, the stabilization via reduction of $\rho_0$ gives way to the instability resulting from the perturbation of the drag force due to the radius change of the flux tube. A corresponding stabilization does not occur for strong upflows because for sufficiently large $\rho_0$ the tube actually contracts at the crests of the displacement and expands at the throughs, so that the perturbation of the drag force again becomes destabilizing.

### 5.5. General case: oscillatory instability

The inclusion of the drag force renders the linear stability problem non-selfadjoint. For a wave-like solution, a phase shift between $\xi_t$ and $\xi_n$ differing from $\pm\pi/2$ removes the symmetry of the force perturbations with respect to the equilibrium position of the flux tube. Consequently, we also may have oscillatory

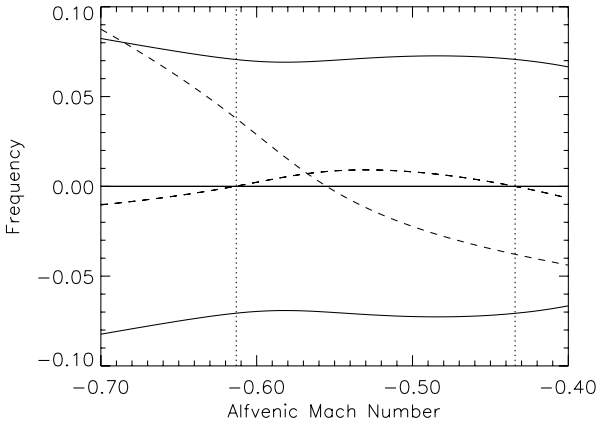


**Fig. 3.** Mode structure in the range of downflow speeds that support oscillatory instability (overstability) for $k = 0.05$. All other parameters are the same as in the foregoing figures. The full and dashed lines give the real and imaginary parts, respectively, of the (dimensionless) mode frequency, $\omega$, as functions of the Alfvénic Mach number, $M_A$, of the perpendicular external flow. Two oscillatory modes [$\mathrm{Re}(\omega) \neq 0$] with equal $\mathrm{Im}(\omega)$ become unstable in the range $-0.61 < M_A < -0.43$ (between the vertical dotted lines). A monotonic mode [$\mathrm{Re}(\omega) = 0$] becomes unstable for $M_A < -0.56$.

instability (overstability) in addition to the monotonic modes. In fact, we find such modes in our case, albeit generally with much smaller growth rates than those of the monotonic modes. Figure 3 shows the mode frequencies for the relevant range of downflow speeds. Here we have taken $k = 0.05$, while all other parameters are the same as in the case shown in Fig. 1. There are two oscillatory modes, which become unstable in the range between the vertical dotted lines ($-0.61 < M_A < -0.43$); both modes have the same growth rate, so that their superposition leads to a standing wave with growing amplitude (overstability). The other two modes are monotonic, i.e., $\mathrm{Re}(\omega) = 0$; one of them becomes unstable for $M_A < -0.56$, while the other mode is always strongly damped (outside the range of the plot).

If we set $\mu = 1$ and $R = 0$ in the dispersion relation, Eq. (23), we can derive an analytic condition for the existence of overstable modes. The resulting biquadratic equation has complex roots if $c_2^2/4 - c_0 < 0$. Because the square root has to be taken

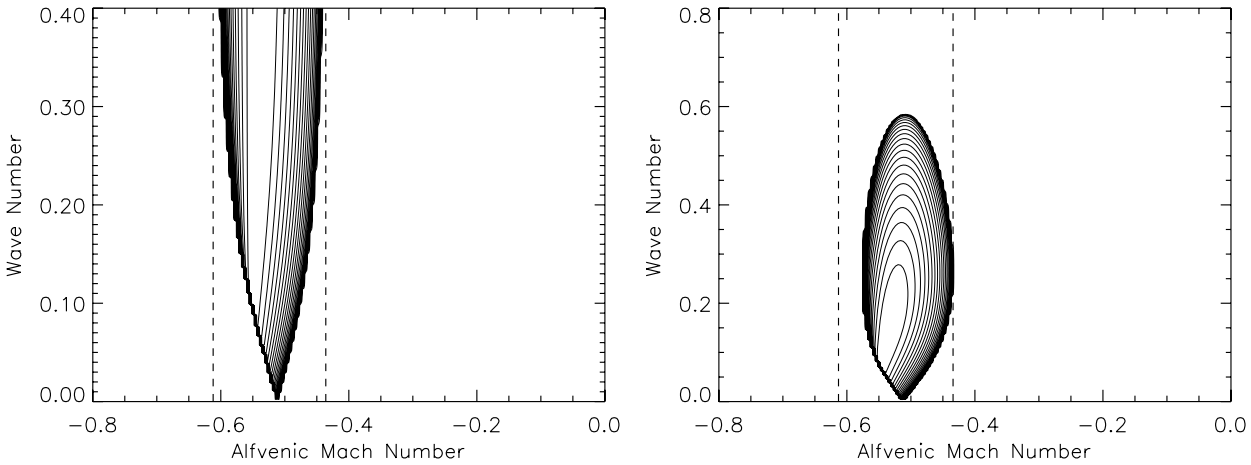


**Fig. 4.** Case $R = 0$: contour lines of equal growth rate of overstable modes, $\mathrm{Im}(\omega) > 0$ and $\mathrm{Re}(\omega) \neq 0$, in the $M_\mathrm{A}$-$k$ plane for $\mu = 1$ (*left panel*) and $\mu = 2$ (*right panel*), respectively. All other parameters correspond to the case shown in the previous figures. The vertical dashed lines indicate the range of Alfvénic Mach numbers ($-0.61 < M_\mathrm{A} < -0.43$) for which the criterion given by Eq. (32) predicts oscillatory instability for sufficiently large values of $k$. While the system remains unstable for arbitrarily large wave numbers in the case $\mu = 1$, there is only a finite range of unstable wave numbers for $\mu = 2$. For small wave numbers, both cases essentially give the same results. The domain of instability always keeps a finite (albeit small) distance from $k = 0$.

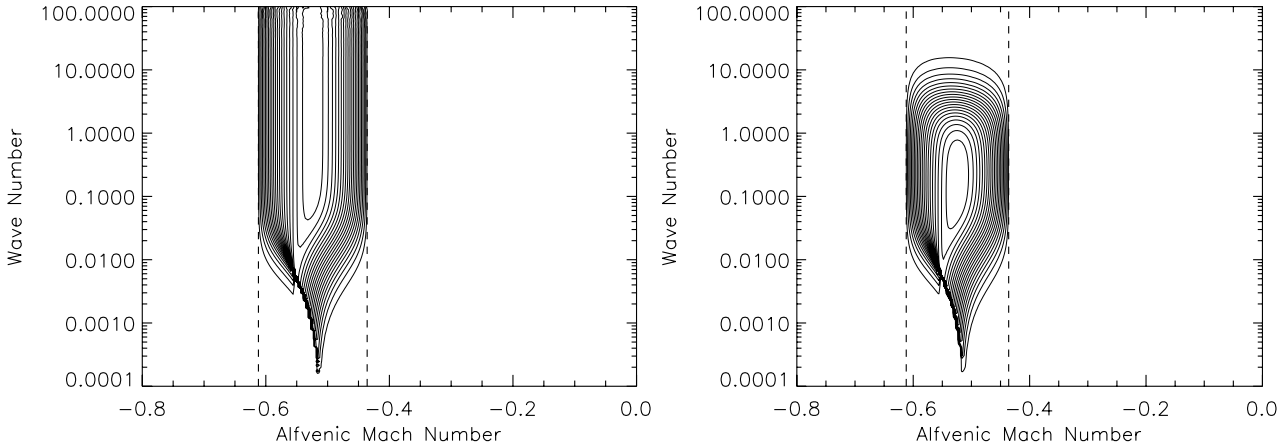


**Fig. 5.** Same as Fig. 4, but with values of $R$ consistently determined from Eq. (22), for $\mu = 1$ (*left panel*) and $\mu = 2$ (*right panel*), respectively. A logarithmic scaling for $k$ has been chosen since the range of relevant wave numbers is much larger than in the case $R = 0$. Oscillatory instability sets in for smaller values of $k$ than for $R = 0$, but the general properties of the instability domains are similar to those shown in Fig. 5. In particular, the range of downflow speeds for which oscillatory instability occurs is the same as in the case $R = 0$ and $\mu = 1$ (dashed vertical lines).

twice to obtain $\omega$, meeting this condition is equivalent to the existence of a pair of overstable modes. The condition can be written in the form

$$0 > \frac{c_2^2}{4} - c_0 = k^2 \left[ \frac{(\beta\chi)^2}{2} - \frac{3\beta\chi}{\gamma} + \frac{4}{\gamma^2} \right] + \frac{1}{4} \left[ -\frac{2}{\gamma} \left( \frac{1}{\gamma} - \frac{1}{2} \right) + \beta\delta + \beta I + \beta D \right]^2 . \quad (32)$$

If the term in the first square brackets on the r.h.s is negative, the condition is fulfilled for sufficiently large values of $k$. Note that this result holds for any value of the external superadiabaticity, $\delta$, because $k$ can be made arbitrarily large (within the limits set by the thin flux tube approximation). The term is negative for $\beta\chi$ in the range $2/\gamma < \beta\chi < 4/\gamma$. For the parameters of our example case, this corresponds almost exactly to the range of Alfvénic Mach numbers for which oscillatory instability instability occurs: $-0.61 < M_\mathrm{A} < -0.43$ (indicated by the vertical dotted lines in Fig. 3). For $\mu > 1$, the terms proportional to $k^4$ in $c_2^2/4 - c_0$ do not cancel, so that the condition for oscillatory instability is only fulfilled in a finite range of wavelengths. This is illustrated in Fig. 4.

It is of course inconsistent to set $R = 0$ and keep the other velocity-related terms at the same time. We have only done so because the range of downflow velocities within which overstable modes are possible in the case $R = 0$, namely, $2/\gamma < \beta\chi < 4/\gamma$, carries over to the general case as well. This can be seen in Fig. 5, which shows the same cases as Fig. 4, but for values of $R$ consistent with Eq. (22). Moreover, the mode structure for fixed $M_\mathrm{A}$ and small values of $k$ near the onset of the oscillatory instability is very similar in both cases as shown in Fig. 6, which also illustrates that the overstable modes evolve from monotonically unstable modes if the wavenumber exceeds a critical value. These monotonic modes, at least in the case $R = 0$, do not follow from the sufficient criterion $c_0 < 0$, indicating that the latter does not represent a necessary criterion as well. The growth rates of the overstable modes in the case $R = 0$ are generally about one order of magnitude larger than for the (realistic) case $R \neq 0$. The monotonic instabilities for sufficiently large values of $M_\mathrm{A}$ (see, e.g., Fig. 1) grow still another order of magnitude faster.

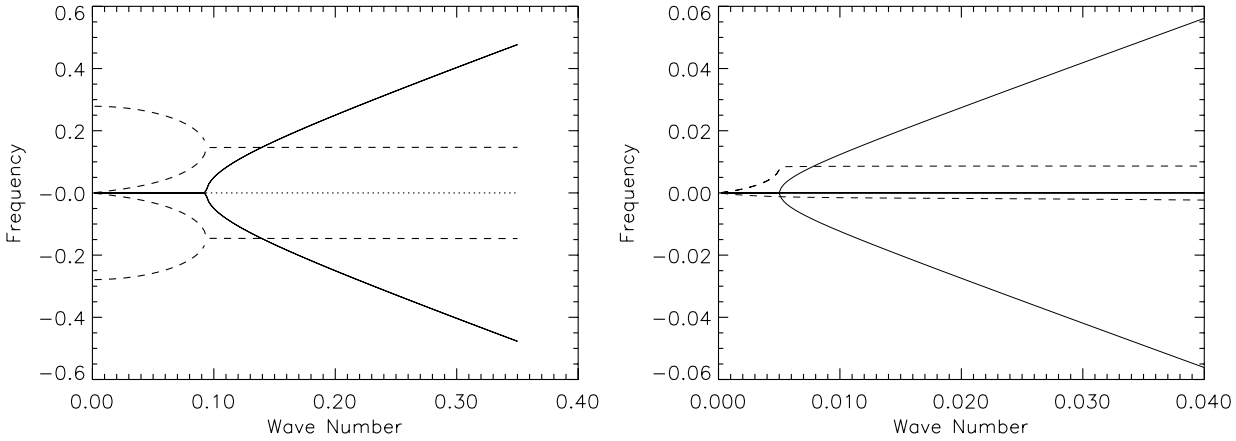


**Fig. 6.** Mode frequencies [full lines: Re($\omega$), dashed lines: Im($\omega$)] as a function of wave number for $M_A = -0.55$. In the case $R = 0$ (*left panel*), there are 4 monotonic modes (2 stable, 2 unstable) for $k < 0.094$, which are transformed into two pairs of oscillatory modes (again 2 stable, 2 unstable) for $k > 0.094$. For both pairs of oscillatory modes, we have $\mathrm{Re}(\omega_1) = -\mathrm{Re}(\omega_2)$ and $\mathrm{Im}(\omega_1) = \mathrm{Im}(\omega_2)$, so that they represent damped and excited standing waves, respectively. For $R \neq 0$ (*right panel*), the symmetry with respect to the horizontal axis is no longer valid but the mode structure is basically the same: 4 monotonic modes (2 stable, 2 unstable) for $k < 0.005$ and two pairs of oscillatory modes for $k > 0.005$. The overstable modes again correspond to a standing wave with growing amplitude. Note that the growth rates are about one order of magnitude smaller for the case $R = 0$.

## 6. Conclusions

We have shown that external flows can drive monotonic as well as oscillatory instability of otherwise stable magnetic flux tube equilibria. The range of flow-driven overstable modes typically extends to much smaller wavelengths than those for which the buoyancy-driven monotonic Parker instability occurs (cf. Spruit & van Ballegooijen 1982; Ferriz-Mas & Schüssler 1993, 1995). The physical mechanism of the flow-induced instabilities is related to a) the effect of the inertial force (gradient of the dynamical pressure) on the external pressure stratification, and b) the changes of the aerodynamic drag force experienced by the displaced flux tube.

Since only the relative motion of flux tube and environment is relevant for the analysis, the stability results can also be applied to buoyantly rising flux tubes (setting $I = 0$). In the case of a Parker instability with long wavelength, the flow instability could the lead to growing secondary loops of smaller wavelength.

Under conditions relevant for the bottom of the solar convection zone, namely $\beta \simeq 10^5 - 10^7$, $|\delta| \simeq 10^{-5} - 10^{-7}$, flow-induced instability typically requires Alfvénic Mach numbers of the order $M_A \simeq 0.1 - 1$. In the case of convective flows, this means that flux tubes with field strengths up to ten times the equipartition field strength (of about $10^4$ G in the lower solar convection zone) can be affected by such instability. This could be relevant for the storage and emergence of magnetic flux in magnetically active cool stars and potentially also for the dynamo process generating the magnetic flux in the first place (e.g., Ferriz-Mas et al. 1994).

More quantitative statements require further detailed analysis, including the effects of spherical geometry, rotation, and meridional flow. This will be the subject of subsequent papers.

## References

Batchelor, G. K. 1967, An Introduction to Fluid Dynamics (Cambridge University Press)
Cheung, M. C. M., Moreno-Insertis, F., & Schüssler, M. 2006, A&A, 451, 303
Defouw, R. J. 1976, ApJ, 209, 266
Emonet, T., Moreno-Insertis, F., & Rast, M. P. 2001, ApJ, 549, 1212
Ferrari, A. 1998, ARA&A, 36, 539
Ferriz-Mas, A., Schmitt, D., & Schüssler, M. 1994, A&A, 289, 949
Ferriz-Mas, A., & Schüssler, M. 1989, Geophys. Astrophys. Fluid Dyn., 48, 217
Ferriz-Mas, A., & Schüssler, M. 1993, Geophys. Astrophys. Fluid Dyn., 72, 209
Ferriz-Mas, A., & Schüssler, M. 1995, Geophys. Astrophys. Fluid Dyn., 81, 233
Hanasz, M., & Lesch, H. 2001, Space Sci. Rev., 99, 231
Kolesnikov, F., Bünte, M., Schmitt, D., & Schüssler, M. 2004, A&A, 420, 737
Moreno-Insertis, F., Schüssler, M., & Ferriz-Mas, A. 1992, A&A, 264, 686
Moreno-Insertis, F., Schüssler, M., & Ferriz-Mas, A. 1996, A&A, 312, 317
Parker, E. N. 1975, ApJ, 198, 205
Parker, E. N. 1979, Cosmical magnetic fields: Their origin and their activity (Oxford: Clarendon Press)
Roberts, B., & Webb, A. R. 1978, Sol. Phys., 56, 5
Ryutov, D. D., & Ryutova, M. P. 1976, J. Exp. Theor. Phys./JETP, 43, 491
Schüssler, M. 1990, in Solar Photosphere: Structure, Convection and Magnetic Fields, IAU Symposium 138, ed. J. O. Stenflo (Dordrecht: Kluwer), 161
Schmitt, D. 1998, Geophys. Astrophys. Fluid Dyn., 89, 75
Schramkowski, G. P. 1996, A&A, 308, 1013
Schramkowski, G. P., & Torkelsson, U. 1996, A&ARev, 7, 55
Schüssler, M. 1984a, in The Hydromagnetics of the Sun (European Space Agency, ESA SP-220), 67
Schüssler, M. 1984b, A&A, 140, 453
Schüssler, M. 1990, Habilitationsschrift, Universität Göttingen, [arXiv:astro-ph/0506050]
Spruit, H. C. 1981, A&A, 102, 129
Spruit, H. C., & van Ballegooijen, A. A. 1982, A&A, 106, 58
van Ballegooijen, A. A., & Choudhuri, A. R. 1988, ApJ, 333, 965
Vishniac, E. T. 1995, ApJ, 451, 816